A Letters Journal Exploring the Frontiers of Physics

December 2020

EPL, **132** (2020) 50003 www.epljournal.org
doi: 10.1209/0295-5075/132/50003

# Stochastic resetting antiviral therapies prevent drug resistance development

A. M. Ramoso[1], J. A. Magalang[1], D. Sánchez-Taltavull[2], J. P. Esguerra[1] and É. Roldán[3]

[1] *Theoretical Physics Group, National Institute of Physics, University of the Philippines - Diliman, Quezon City 1101, Philippines*
[2] *Visceral Surgery and Medicine, Inselspital, Bern University Hospital, Department for Biomedical Research, University of Bern - Murtenstrasse 35, 3008 Bern, Switzerland*
[3] *ICTP - The Abdus Salam International Centre for Theoretical Physics - Strada Costiera 11, 34151, Trieste, Italy*

received 18 September 2020; accepted in final form 18 November 2020
published online 30 December 2020

PACS 05.40.-a – Fluctuation phenomena, random processes, noise, and Brownian motion
PACS 87.16.-b – Subcellular structure and processes

**Abstract** – We study minimal mean-field models of viral drug resistance development in which the efficacy of a therapy is described by a one-dimensional stochastic resetting process with mixed reflecting-absorbing boundary conditions. We derive analytical expressions for the mean survival time for the virus to develop complete resistance to the drug. We show that the optimal therapy resetting rates that achieve a minimum and maximum mean survival times undergo a second- and first-order phase transition-like behaviour as a function of the therapy efficacy drift. We illustrate our results with simulations of a population dynamics model of HIV-1 infection.



Antiviral and antiretroviral therapies are continuously being developed to tackle viral diseases [1]. Because of viral evolution, a therapy that is effective today may not remain effective forever [2]. This process is known as drug resistance development and it is of special importance in chronic infections such as HIV-1 [3–5], and also for herpes and hepatitis [6]. Viral evolution results in an increase in the number of infected cells, leading to a failure of the normal functions of the infected patient that can result in their death [2]. Because viruses replicate and mutate rapidly, and mutation is a random process, viral evolution is intrinsically noisy [7,8]. When possible, practitioners overcome this situation by changing the therapy given to the patient. Changes in antiviral therapies can occur because of a detected viral resistance [3,9], or for purely stochastic reasons, *e.g.*, the appearance in the market of a therapy that is cheaper or has less secondary effects. It remains an open yet challenging problem to characterize and design therapy change protocols that ensure large patient survival times that are robust to drug resistance fluctuations.

Stochastic models have been used to study viral evolution [7–11]. Examples include the use of branching processes to describe viral persistence and extinction [7,8], and population dynamics models to assess the impact of a treatment in drug resistance development in the context of HIV-1 [12]. A model that described RNA virus evolution as a diffusion process in a fitness landscape [13] was able to explain the experimentally observed rapid initial growth followed by a slower stage of linear growth in the logarithm of fitness of clone colonies of vesicular stomatitis virus [14,15]. In the same vein, the notion of a fluctuating therapy efficacy can be used to describe the evolution of therapy protocols.

Viral evolution can be modelled as a stochastic diffusion process involving incremental changes in efficacy —due to viral mutation— punctuated by sudden changes in efficacy —due to changes in therapy. Diffusions with stochastic resetting [16–27] thus provide a promising framework to model therapy evolution. This framework has been instrumental to describe biophysical processes with sudden changes, namely RNA polymerase backtracking [28,29], receptor dynamics [30], cell crawling [31], and population dynamics [32–41]. See [17] for a review of applications.

Stochastic resetting has been discussed previously in the context of population dynamics. In prey-predator models, resetting accounts for the tendency of predators to return to a preferred site [32]. Ohta-Kimura continuous-ladder models of population genetics have been shown to be analogous to diffusions with stochastic resetting [33].

In birth-death processes, stochastic resetting represents a catastrophe where a population size changes all of a sudden [34–41]. It remains unclear how in multiscale processes stochastic resetting of a slow variable (*e.g.*, a therapy efficacy) affects a fast variable describing the dynamics of a time-varying population (*e.g.*, cells and viruses).

In this letter, we introduce a stochastic resetting model for the evolution of the efficacy of an antiviral therapy, and study its evolution under different treatment protocols. We first describe the therapy efficacy as a one-dimensional resetting biased diffusion model with mixed absorbing and reflecting boundaries, calculate an exact analytical expression for the mean first-passage time, and test our result by comparing it with Langevin dynamics simulations. We then discuss the clinical effects of our viral evolution model by coupling the stochastic-resetting biased-diffusion therapy efficacy to a population dynamics model of HIV-1 chronic disease.

We describe the efficacy of an antiviral treatment as a bounded stochastic process $0 \leq \eta(t) \leq 1$ where $\eta = 0$ and $\eta = 1$ correspond to a completely ineffective and completely effective therapy, respectively. We assume that treatments that stop working lead to the death of the patient, *i.e.*, $\eta = 0$ is an absorbing boundary. On the other hand $\eta = 1$ is a reflecting boundary set at the maximum 100% therapy efficacy. We model the evolution of therapy efficacy $\eta(t)$ as a biased random walk or drift-diffusion process in "efficacy space" with diffusion coefficient $D$ and drift $v$. The therapy is often biased in the direction of lesser efficacy, *i.e.*, the drift is negative $v < 0$, due to the fact that viruses develop resistance to the existing therapies that survive in the long run. Furthermore, we complement the biased diffusion model with a resetting protocol that switches the therapy efficacy to a value $\eta_0$ instantaneously at random Poissonian times with rate $r$. Such therapy "resetting" events can be due to the introduction of a new dose of drug, the discovery of more effective variants of the therapy, etc. See fig. 1 for an illustration of the model and a sample stochastic trajectory of the therapy efficacy.

The evolution of the model can be described by the Fokker-Planck equation with source terms

$$\partial_t P + \partial_\eta (vP - D\partial_\eta P) = -rP + r\delta(\eta - \eta_0), \qquad (1)$$

where $P \equiv P(\eta, t \,|\, \eta_0, 0)$ is the conditional probability density that the therapy is at $\eta$ at time $t$ given that its initial value (at which it is reset at rate $r$) was $\eta_0$. The dynamics is complemented by an absorbing boundary condition at $\eta = 0$, $\lim_{\eta \to 0^+} P(\eta, t) = 0$ and a zero-flux reflecting boundary condition at $\eta = 1$, $J(1, t) = 0$ where $J(\eta, t) = vP(\eta, t) - D\partial_\eta P(\eta, t)$ is the probability current.

In the following, we derive analytical expressions for the finite-time survival probability and the mean survival time. We denote by *survival time* the first-passage time of the therapy efficacy to reach the absorbing boundary

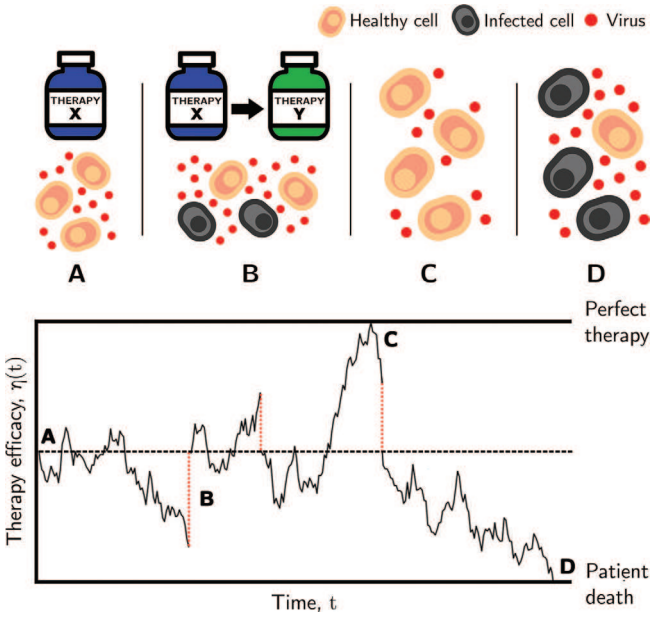


Fig. 1: Illustration of the stochastic resetting model of antiviral therapy efficacy. Top: sketch of the main ingredients of the model. Bottom: sample trajectory of the therapy efficacy as a function of time, with A–D illustrating key events during a single realization of the process. A) Initial condition, for a 50% efficient therapy $\eta_0 = 1/2$. B) Change of the current therapy at a random time (stochastic resetting) by a new one with 50% efficacy. C) Reflecting boundary condition modelling the maximum possible therapy efficacy $\eta = 1$. D) Absorbing boundary condition yielding to the death of the patient due to a completely inefficient therapy $\eta = 0$.

$\eta = 0$. To this aim, we first make use of a relation between the finite-time survival probability with resetting $S_r(\eta_0, t)$ and the survival probability without resetting $S_0(\eta_0, t)$ [17,20,42]

$$S_r(\eta_0, t) = e^{-rt} S_0(\eta_0, t) + r \int_0^t \mathrm{d}\tau e^{-r\tau} S_0(\eta_0, \tau) S_r(\eta_0, t - \tau). \qquad (2)$$

From eq. (2) we use the relation $\tilde{F}_r(\eta_0, s) = 1 - s\tilde{S}_r(\eta_0, s)$ and show that the Laplace transform of the first-passage probability with resetting $\tilde{F}_r(\eta_0, s)$ and without resetting $\tilde{F}_0(\eta_0, s)$ are related through the identity (see the Supplementary Material `Supplementarymaterial.pdf` (SM))

$$\tilde{F}_r(\eta_0, s) = \frac{(r + s)\tilde{F}_0(\eta_0, s + r)}{s + r\tilde{F}_0(\eta_0, s + r)}. \qquad (3)$$

We show that the Laplace transform of the first-passage probability without resetting is given by [43]

$$\tilde{F}_0(\eta_0, s) = e^{-\frac{\eta_0 v}{2D}} \frac{2D\omega \cosh[\omega(\eta_0 - 1)] + v \sinh[\omega(\eta_0 - 1)]}{2D\omega \cosh \omega - v \sinh \omega}, \qquad (4)$$

where $\omega = \sqrt{v^2 + 4Ds}/(2D)$. Substituting eq. (4) in eq. (2) and using the relation $\langle \tau_r \rangle = -\partial_s \tilde{F}_r(\eta_0, s)|_{s=0}$

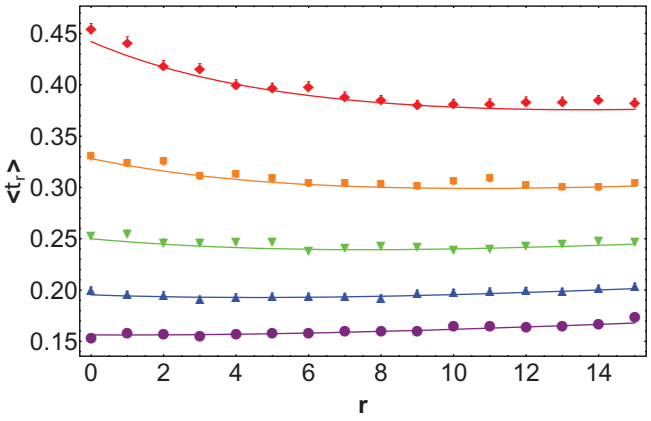


Fig. 2: Mean survival time for a therapy to become completely inefficient, as a function of the therapy resetting rate: numerical simulations (symbols) and analytical results (lines) given by eq. (5). The data correspond to parameter values diffusion $D = 1.5$, initial efficacy $\eta_0 = 1/2$ and different values of drift $v$: $v = 2$ (♦), $v = 1$ (■) $v = 0$ (▼), $v = -1$ (▲), and $v = -2$ (●). For all parameter values, the simulations were done using Euler's numerical integration with parameters: $10^5$ number of simulations, each with time step $\Delta t = 10^{-5}$ and total simulation time $t_{\rm sim} = 10^6$.

we obtain the following analytical expression for the mean first-passage time:

$$\langle \tau_r \rangle = \frac{\phi(\mathrm{Pe}, \Omega, \eta_0)}{r\{\mathrm{Pe}\sinh[\Omega(\eta_0 - 1)] + \Omega\cosh[\Omega(\eta_0 - 1)]\}^2}, \tag{5}$$

where the non-trivial function $\phi(\mathrm{Pe}, \Omega, \eta_0) = \mathrm{Pe}^2\{e^{\eta_0\,\mathrm{Pe}}\cosh[\Omega(\eta_0 - 2)] - \cosh[2\Omega(\eta_0 - 1)]\} + \mathrm{Pe}\Omega\{e^{\eta_0\,\mathrm{Pe}}\sinh[\Omega(\eta_0 - 2)] - \sinh[2\Omega(\eta_0 - 1)]\} + \xi\{e^{\eta_0\,\mathrm{Pe}}\cosh[\Omega\eta_0] - \cosh[2\Omega(\eta_0 - 1)] + e^{\eta_0\,\mathrm{Pe}}\cosh[\Omega(\eta_0 - 2)] - 1\}$ depends on the model parameters through the dimensionless quantities $\mathrm{Pe} = v/(2D), \Omega = \sqrt{v^2 + 4Dr}/(2D)$, and $\xi = r/(2D)$.

Figure 2 shows an excellent agreement between eq. (5) and numerical Langevin dynamics simulations of the model, for different parameter values. For positive values of $v$, the mean survival time decreases monotonously with the therapy resetting rate, hence it is beneficial to switch slowly among beneficial therapies (*i.e.*, keeping $r$ small) in order to maximize the survival time. For small and even negative values of the efficacy drift, the mean first-passage time is non monotonous; the minimum average survival time takes place for intermediate values of $r$. For therapies with large negative bias $v < 0$, a case that is relevant in the context of viral evolution, $\langle \tau_r \rangle$ increases monotonically with $r$, *i.e.*, the maximum average survival is achieved switching the therapies as frequently as possible.

In a real-world scenario, practitioners have to deal with limited resources such as a finite number of therapies during the life of a patient. Within this scenario, it is important to know what the optimal resetting rate is which achieves a desired value of the mean survival time of the

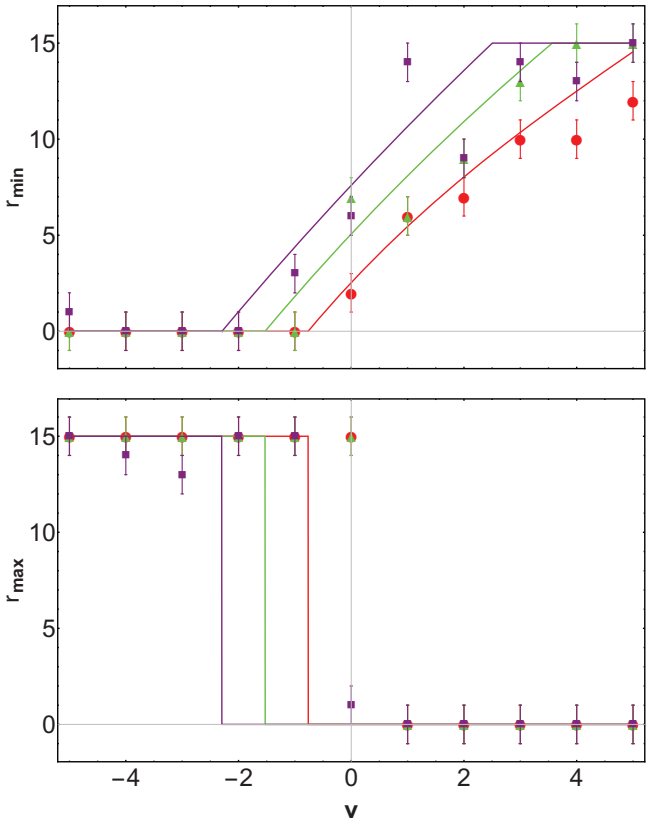


Fig. 3: Comparison between simulations (symbols) and theoretical results (lines) of optimal resetting rates as a function of the therapy efficacy drift: $r_{\rm min}$ (top) and $r_{\rm max}$ (bottom) denote the value of the resetting rate at which the mean survival time attains its minimum and maximum values, respectively. The different curves and symbols are obtained by imposing a maximum allowed resetting rate of 15, for different values of $v$ and $D = 0.5$ (●, red line), $D = 1$ (▲, green line) and $D = 1.5$ (■, purple line). The rest of the simulation parameters are set to the same values as in fig. 2.

patient. To study this problem, we evaluate in fig. 3 the resetting rates $r_{\rm min}$ and $r_{\rm max}$ for which the mean survival time attains respectively its minimum and maximum value, within a finite range of resetting rate. We find that $r_{\rm min} = 0$ for rapidly evolving virus ($v$ large and negative), whereas $r_{\rm min}$ increases monotonously with $v$ for larger values. Notably $r_{\rm min}$ presents a non-analyic behaviour at a critical value of $v$, and hence of the Peclet number, as reported by recent work on drift-diffusion processes with one absorbing boundary [26]. On the other hand, our results show that the "optimal" resetting rate $r_{\rm max}$ achieving the maximum mean survival time displays a dependency with the therapy drift that has reminiscences of a first-order phase transition; it exhibits a sudden jump from the maximum allowed resetting rate (for rapidly evolving virus) to zero. Such transition occurs at a critical value of $v$ that depends on the fluctuations $D$ of the therapy efficacy; it can take place at biologically relevant values ($v$ negative) when $D$ is large enough.

We now consider a stochastic mean-field population dynamics model describing a multicellular organism containing healthy $H$, latent $L$, and productively infective $I$ cells by a chronic viral disease such as HIV-1. The state of the system is described by its time-dependent numbers $H$, $I$ and $L$, whose dynamics is driven by the stochastic resetting therapy efficacy $\eta$. We remark that we include in the model a population of latent cells to account for a chronic infection, inspired by previous mathematical models of HIV-1 [4]. The dynamics of the model is given by three coupled ordinary differential equations (eqs. (6)–(8) below) driven by an autonomous stochastic differential equation (eq. (9) below):

$$\frac{\mathrm{d}H}{\mathrm{d}t} = \alpha - \lambda_H H - (1-\eta)\beta H I, \tag{6}$$

$$\frac{\mathrm{d}L}{\mathrm{d}t} = \epsilon(1-\eta)\beta H I + pL\left(1-\frac{L}{K}\right) - a_L L - \lambda_L L, \tag{7}$$

$$\frac{\mathrm{d}I}{\mathrm{d}t} = (1-\epsilon)(1-\eta)\beta H I + a_L L - \lambda_I I, \tag{8}$$

$$\mathrm{d}\eta = (1-\chi)(v\mathrm{d}t + \sqrt{2D}\mathrm{d}W) + \chi(\eta_0 - \eta). \tag{9}$$

Here, $\alpha$ denotes the rate of recruitment of new healthy cells, $\lambda_H$ is the death rate of healthy cells, $\beta$ is the infection rate, $\epsilon$ is the probability of an infection resulting into a latent cell, $p$ is the proliferation rate of latent infected cells, $K$ is the carrying capacity which introduces a logistic growth, $a_L$ the activation rate of latent cells, $\lambda_L$ death rate of latent cells, and $\lambda_I$ the death rate of infected cells. Note that the infection rate $\beta$ is multiplied by the instantaneous probability $(1-\eta)$ of the infection to occur. Finally, $\chi$ is a binary variable which is equal to one (zero) when a reset occurs (does not occur) with probability $r\mathrm{d}t$ $(1-r\mathrm{d}t)$, and $W$ is the Wiener process. Hence, eq. (9) complemented with mixed absorbing boundary conditions describes the previously introduced therapy efficacy stochastic model. Further details of the model can be found in the SM.

Next, we illustrate the model with numerical simulations showing the impact of the therapy efficacy in the number of healthy cells of a patient. For this purpose we numerically integrate eqs. (6)–(9). In this case, we only consider therapies with $v < 0$ because mutations beneficial to the virus are dominant in its evolution. When changes in therapy are not allowed we observe a drift in $\eta$ through the absorbing barrier, followed by the healthy cells (fig. 4, top). Under stochastic changes in the therapy $\eta$ still drifts through the absorbing state barrier, however, after the stochastic reset, we often observe a period in which the healthy cells recover, delaying the absorption time of $\eta$ (fig. 4, bottom). We remark that, when $\eta$ reaches the absorbing boundary at zero, the cell population still evolves, towards its fixed point. Note that, unlike in our first model, we allow here for resets from $\eta = 0$ to $\eta_0$ because even in the absence of therapy the patient can survive until their therapy changes. This motivates us to study first-passage times in the context of healthy cells. In doing so, we define the *patient survival time* as the time elapsed until $H \leq \alpha/(2\lambda_H)$, which corresponds to the time until it falls below half of the fixed point in the absence of infection.

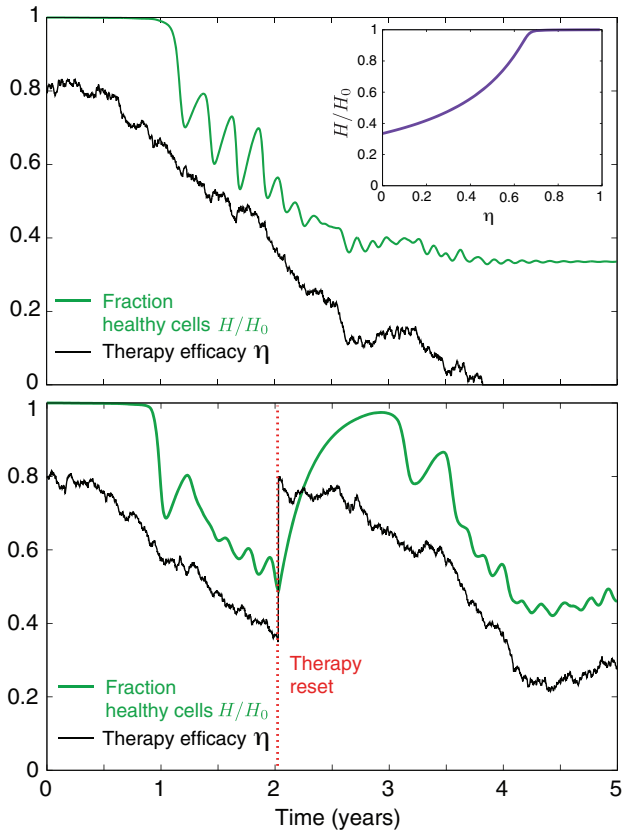


Fig. 4: Numerical simulations of the viral evolution population-dynamics model given by eqs. (6)–(9) in the absence (top) and in the presence (bottom) of therapy resetting: fraction of healthy cells with respect to the initial value $H/H_0$ (green line) and therapy efficacy (black line) as a function of time. The inset in the top panel shows the average fraction of healthy cells as a function of the therapy efficacy in the absence of resetting, and the red dashed line in the bottom panel illustrates the time at which the antiviral therapy efficacy is restored to its initial value. Parameters of the simulations: $v = -3\times10^{-4}\,\mathrm{days}^{-1}$ and $D = 10^{-5}\,\mathrm{days}^{-1}$, $\alpha = 6000\,\mathrm{days}^{-1}\,\mathrm{ml}^{-1}$, $\lambda_H = 0.01\,\mathrm{days}^{-1}$, $\beta = 5\times10^{-6}\,\mathrm{ml\ days}^{-1}$, $\epsilon = 0.01$, $p = 0.2\,\mathrm{days}^{-1}$, $a_L = 0.1\,\mathrm{days}^{-1}$, $\lambda_L = 0.01\,\mathrm{days}^{-1}$, $\lambda_I = 1\,\mathrm{days}^{-1}$, $K = 100\,\mathrm{cells\ ml}^{-1}$, with $r = 0$ (top) and $r = (1/3)\,\mathrm{years}^{-1}$ (bottom), with initial condition $\eta_0 = 0.8$, $H_0 = 6\times10^5\,\mathrm{cells\ ml}^{-1}$, $L_0 = 1\,\mathrm{cells\ ml}^{-1}$, $I_0 = 0\,\mathrm{cells\ ml}^{-1}$, and step size $\Delta t = 1\,\mathrm{days}$. The inset (in the top panel) shows the value of $H$ at the non-trivial fixed point of the system eqs. (6)–(8) for a fixed value of $\eta$.

We now determine the impact of changes in the therapy in a region of parameters for $v$ and $D$. Figure 5 shows the mean survival time (left panels) and the mean patient survival time (right panels) as a function of $v$ and $D$ obtained from analytical and numerical calculations. For the parameter values studied here, the resetting of therapies increases both the mean survival time and the

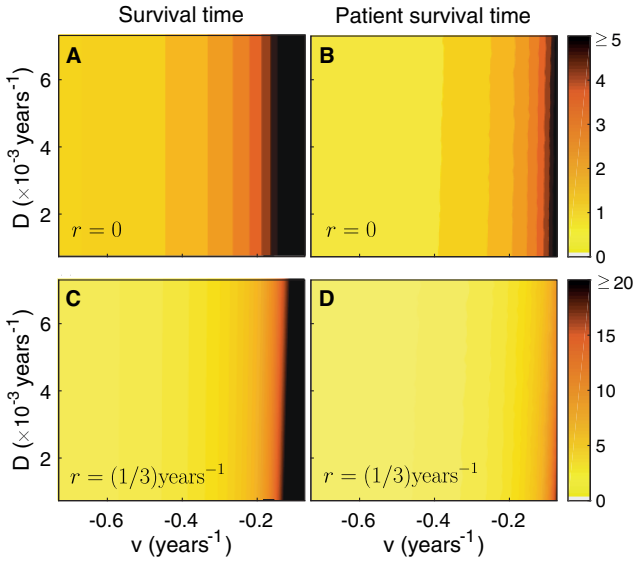


Fig. 5: Mean survival times (in years) as a function of the therapy efficacy drift $v$ and diffusion $D$. (A), (C): analytical value of the mean first-passage time for the therapy efficacy $\eta$ to reach the absorbing boundary $\eta = 0$, given by eq. (5). (B), (D): numerical value of the mean time elapsed until the fraction of healthy cells falls below 1/2 its initial value ((B), (D)). The color maps show the values obtained for resetting rates $r = 0$ ((A), (B)) and $r = (1/3)\,\text{years}^{-1}$ ((C), (D)). In (B), (D) the values of the simulation parameters were set to the same values as in fig. 4 except the time step $\Delta t = 0.01$ days, and the averages are done over 2000 numerical simulations of eqs. (6)–(9).

mean patient survival time. Their qualitative behaviour is similar: when the drug resistance develops slowly ($v$ negative but small) the survival time and the patient survival time are large, and vice versa. The larger the resistance fluctuations $D$, the lower the survival times, however this dependency is weaker than for $v$. Notably, when executing therapy resets at a rate of $(1/3)\,\text{years}^{-1}$, the mean patient survival time can exceed 20 years for small values of $v$ and $D$ (fig. 5(D)).

We have introduced a multiscale stochastic model linking drug resistance development described by a one-dimensional stochastic resetting process with cell population dynamics. The coupling of the biased stochastic resetting therapy to a mean-field population dynamics model provides novel insights to mathematical modelling of drug resistance development. Our model and techniques enable to estimate the number of healthy cells and the patient survival time in a chronic disease, *e.g.*, HIV-1. Our analytical and numerical results quantify the beneficial aspects of therapy changes at random Poissonian times for the mean survival time of a patient as a function of the viral evolution parameters. We have derived an analytical expression for the mean survival time of the stochastic resetting therapy efficacy as a function of its drift and diffusivity. This expression can be used to estimate patient survival times in some limits. It will be interesting to extend our work to, *e.g.*, compare different therapy resetting protocols under time constraints, account for drug resistance development which depends on the instantaneous viral load, account for multiple therapies [44], etc. We expect potential applications of our work to determine the epidemiological impact of drug resistance development, using models where the immunity to certain drugs can be transported between individuals.

* * *

We thank Arnab Pal for useful feedback on our preprint.

REFERENCES

[1] Lichterfeld M. and Zachary K. C., *Ther. Adv. Chronic Dis.*, **2** (2011) 293.
[2] Clutter D. S., Jordan M. R., Bertagnolio S. and Shafer R. W., *Infect. Genet. Evol.*, **46** (2016) 292.
[3] Pillay D. and Zambon M., *Br. Med. J.*, **317** (1998) 660.
[4] Perelson A. S. and Nelson P. W., *SIAM Rev.*, **41** (1999) 3.
[5] Sanchez-Taltavull D., Vieiro A. and Alarcon T., *J. Math. Biol.*, **73** (2016) 919.
[6] Strasfeld L. and Chou S., *Infect. Dis. Clin.*, **24** (2010) 809.
[7] Fabreti L. G., Castro D., Gorzoni B., Janini L. M. R. and Antoneli F., *Bull. Math. Biol.*, **81** (2019) 1031.
[8] Manrubia S. C. and Lázaro E., *Phys. Life Rev.*, **3** (2006) 65.
[9] Wensing A. M., Calvez V., Ceccherini-Silberstein F., Charpentier C., Günthard H. F., Paredes R., Shafer R. W. and Richman D. D., *Top. Antivir. Med.*, **27** (2019) 111.
[10] Tria F., Laessig M., Peliti L. and Franz S., *J. Stat. Mech.*, **2005** (2005) P07008.
[11] Nelson M. I. *et al.*, *PLoS Pathog.*, **2** (2006) e125.
[12] Zitzmann C. and Kaderali L., *Front. Microbiol.*, **9** (2018) 1546.
[13] Tsimring L. S., Levine H. and Kessler D. A., *Phys. Rev. Lett.*, **76** (1996) 4440.
[14] Novella I. S., Duarte E. A., Elena S. F., Moya A., Domingo E. and Holland J. J., *Proc. Natl. Acad. Sci. U.S.A.*, **92** (1995) 5841.
[15] Holland J. J., De La Torre J. C., Clarke D. and Duarte E., *J. Virol.*, **65** (1991) 2960.
[16] Evans M. R. and Majumdar S. N., *Phys. Rev. Lett.*, **106** (2011) 160601.
[17] Evans M. R., Majumdar S. N. and Schehr G., *J. Phys. A*, **53** (2020) 193001.
[18] Bhat U., De Bacco C. and Redner S., *J. Stat. Mech.*, **2016** (2016) 083401.
[19] Kuśmierz Ł. and Gudowska-Nowak E., *Phys. Rev. E*, **92** (2015) 052127.
[20] Pal A. and Prasad V., *Phys. Rev. E*, **99** (2019a) 032123.
[21] Pal A. and Prasad V., *Phys. Rev. Res.*, **1** (2019) 032001(R).
[22] Durang X., Lee S., Lizana L. and Jeon J.-y., *J. Phys. A*, **52** (2019) 224001.

[23] Christou C. and Schadschneider A., *J. Phys. A*, **48** (2015) 285003.
[24] Pal A. and Reuveni S., *Phys. Rev. Lett.*, **118** (2017) 030603.
[25] Chechkin A. and Sokolov I., *Phys. Rev. Lett.*, **121** (2019) 042128.
[26] Ray S., Mondal D. and Reuveni S., *J. Phys. A*, **52** (2019) 255002.
[27] Basu U., Kundu A. and Pal A., *Phys. Rev. E*, **100** (2019) 032136.
[28] Roldán É., Lisica A., Sánchez-Taltavull D. and Grill S. W., *Phys. Rev. E*, **93** (2016) 062411.
[29] Tucci G., Gambassi A., Gupta S. and Roldán É., arXiv preprint, arXiv:2005.05173 (2020).
[30] Mora T., *Phys. Rev. Lett.*, **115** (2015) 038102.
[31] Bressloff P. C., *Phys. Rev. E*, **102** (2020) 022134.
[32] Mercado-Vásquez G. and Boyer D., *J. Phys. A*, **51** (2018) 405601.
[33] da Silva T. T. and Fragoso M. D., *J. Phys. A*, **51** (2018) 505002.
[34] Levikson B., *J. Appl. Probab.*, **14** (1977) 492.
[35] Pakes A. G., *J. Appl. Probab.*, **15** (1978) 65.
[36] Pakes A. G., *Commun. Stat. Stoch. Models*, **13** (1997) 255.
[37] Brockwell P. J., Gani J. and Resnick S. I., *Adv. Appl. Probab.*, **14** (1982) 709.
[38] Brockwell P. J., *Adv. Appl. Probab.*, **17** (1985) 42.
[39] Kyriakidis E. G., *Stat. Probab. Lett.*, **20** (1994) 239.
[40] Economou A. and Fakinos D., *Eur. J. Oper. Res.*, **149** (2003) 625.
[41] Visco P., Allen R. J., Majumdar S. N. and Evans M. R., *Biophys. J.*, **98** (2010) 1099.
[42] Pal A., Kundu A. and Evans M. R., *J. Phys. A.*, **49** (2016) 225001.
[43] Godec A. and Metzler R., *Phys. Rev. X*, **6** (2016) 041037.
[44] Richman D. D., Margolis D. M., Delaney M., Greene W. C., Hazuda D. and Pomerantz R. J., *Science*, **323** (2009) 1304.